

IMPERIAL COLLEGE LONDON

LIFE SCIENCES

---

## The Role of Temperature-Dependent Human Behaviour and Virus Stability on Respiratory Disease Dynamics

---

*Author:*

Ruth Keane

*Supervisors:*

Dr Samraat Pawar

Dr Michael Tristem



Word Count: 5888

A thesis submitted in partial fulfilment of the requirements for the degree of  
Master of Science at Imperial College London

Formatted in the style of Ecology

Submitted for the MSc in Computational Methods in Ecology and Evolution

27 August 2020

## Abstract

Respiratory viruses can show strong seasonality and are a substantial burden on health services. Understanding their seasonality could help to reduce their impact. Previous models of disease have not explicitly modelled contact rate and the decay rate of the virus simultaneously. I suggest a model for temperature dependent transmissibility based on both viral survival and contact rate to be used in an SEIR model. Using this model and estimated average weekly temperatures, I predict the number of infectious individuals each day for 77 countries (for 10 years, then averaged over one year). As contact rate patterns with climate are not fully understood, I vary the climate at which contact rate is assumed to be highest, resulting in repeats at different levels of mismatch, where mismatch measures the difference between the climates where contact rate and virus survival are highest. To assess which level of mismatch was best, I compare the correlation between influenza data and model results (averaged for one year) for each mismatch for each country. In temperate regions, the best mismatch result was consistent with highest contact rate and virus survival occurring at the same temperature for influenza. In the tropics the mismatch was much more varied and there was a high variability between countries. A mismatch of 0.5 led to lower mean  $R_0$  values and a mismatch of 1 led to lower maximum  $R_0$  values. When I applied this model to COVID-19 (using the best mismatch from influenza results), temperate regions had a consistent winter peak. Shifting the mismatch value decreased the mean and maximum  $R_0$ . This is new model which attempts to provide a mechanistic model for respiratory virus seasonality which could be used to improve current epidemiological methods. More research into the climate-dependence of contact rate is very important in understand how human behaviour might effect seasonal forcing.

# Contents

<b>Abstract</b>	<b>1</b>
<b>1 Introduction</b>	<b>4</b>
<b>2 Methods</b>	<b>9</b>
2.1 Model . . . . .	9
2.2 Paramaterisation . . . . .	12
2.3 Data Sources and Sorting . . . . .	12
2.4 Analytical Sensitivity Analysis . . . . .	13
2.5 Model Simulations . . . . .	14
2.5.1 Sensitivity Analysis in Integration . . . . .	14
2.6 Analysis of Integration Results and Data . . . . .	15
2.7 COVID-19 . . . . .	15
2.8 Statistical Analysis . . . . .	15
<b>3 Results</b>	<b>16</b>
3.1 Models and Data . . . . .	16
3.2 Mismatch and Temperature . . . . .	16
3.3 Sensitivity Analysis . . . . .	17
3.4 Mismatch and Disease Prevalence . . . . .	18
3.5 COVID-19 . . . . .	19
<b>4 Discussion</b>	<b>21</b>
4.1 Temperature Findings . . . . .	21
4.2 Different Climate Variables . . . . .	22
4.3 COVID-19 . . . . .	22
4.4 Limitations and the Future . . . . .	24
<b>5 Conclusion</b>	<b>25</b>
<b>Bibliography</b>	<b>26</b>
<b>Supplementary Information</b>	<b>32</b>
5.1 COVID-19 over the year . . . . .	34

## List of Figures

1	Visual Representation of SEIR model . . . . .	9
2	Visualisation for different levels of mismatch . . . . .	17
3	Temperature box and whisker plot . . . . .	18
4	Sensitivity Analysis Results . . . . .	18
5	Influenza Mismatch and $R_0$ . . . . .	19
6	COVID-19 Mismatch and $R_0$ . . . . .	20
7	Temperature and Humidity . . . . .	23
8	Supplementary Information: Humidity box and whisker plots . . . . .	34
9	Supplementary Information: Variance box and whisker plots . . . . .	35
10	Supplementary Information: $R_0$ over time in different regions . . . . .	36

## List of Tables

1	Basic Parameter meanings for SEIR model. Parameters are described fully (with units and sources) in Table 2 of Supplementary information . . . . .	10
2	Supplementary Information: Table of model parameters . . . . .	32
3	Supplementary Information: Table of parameter values . . . . .	33

# 1 Introduction

Respiratory viruses put a huge burden on the world at both endemic and epidemic levels. Influenzas are a problem both as seasonal influenza and pandemic influenzas such as H1N1 (World Health Organization (WHO) 2018b; World Health Organization (WHO) 2018a). Most recently COVID-19, a respiratory virus caused by SARS-CoV-2 is having significant impacts across the world, first seen in December 2019 and declared a pandemic on the 11th March 2020. (World Health Organization (WHO) 2020b; World Health Organization (WHO) 2020a). Previous coronavirus epidemics such as SARS have prompted discussions about the importance of understanding the nature of seasonality infectious disease but much is still unknown (Dowell and Ho 2004). The future of COVID-19 is uncertain but some predict that repeated wintertime outbreaks are likely, at least in the short term (Kissler et al. 2020). Understanding the causes for the dynamics of these diseases is helpful for planning the timing and types of interventions that should take place. This can be especially important for seasonal pathogens because periods with fewer cases allow time for planning in advance of the next outbreak.

Differences in climate have been frequently linked to disease, both temporally and spatially. In terms of differences over the course of a year, influenza is perhaps the most well known seasonal respiratory virus but others include respiratory syncytial virus (RSV) (J. W. Tang et al. 2010), mild betacoronaviruses (Kissler et al. 2020) pneumococcus and rubella (Dowell and Ho 2004). These tend to peak in the winters of temperate regions. Climate may also mediate difference between severity of outbreaks in different years. In terms of differences in space, in general the tropics and temperate regions have different disease patterns. Marked yearly winter peaks may be more common in temperate regions but in the tropics, disease may peak in the rainy season, have two peaks or remain high all year round (J. D. Tamerius et al. 2013).

For the most part, work to understand the impact of climate is statistical work that links climate with disease including time series analysis. While not being mechanistic these can be very valuable in understanding the factors that lead to seasonality and heterogeneity of disease. A lot of phenomenological work has explored whether COVID-19 is linked to environmental variables. These tend to indicate that lower temperatures and lower relative humidity are associated with more disease but results do vary based on the area and the study methods (*add references/specific examples*). (*add phenomenological flu*) Attempts have been made to demonstrate causality between climate and influenza. Deyle et al. (2016) used convergent cross mapping to find that absolute humidity mediated by temperature was the most likely cause but whether this truly demonstrates causality is in question because the same approach can be used to demonstrate that influenza causes the climatic conditions, which is obviously not the case

32 (Baskerville and Cobey 2017; Sugihara, Deyle, and Ye 2017) . As O. N. Bjørnstad and Viboud (2016)  
33 point out, combination of such work with mechanistic models is important to enable prediction of future  
34 disease.

35 The causes for seasonality have been discussed in lots of detail but can broadly be split into three  
36 potential reasons: human behaviour, human immunity and viral survival (J. Tamerius et al. 2011). Viral  
37 survival during transmission is essential for successful transmission. Numerous studies have explored the  
38 effect of climate variables of survival of viruses in a lab setting and they find that for lipid enveloped  
39 viruses, lower temperatures and lower relative humidities have better virus survival. (Julian W. Tang  
40 2009; J. Tamerius et al. 2011). The effect of temperature on influenza is reviewed by Irwin et al. (2011)  
41 who found that across air, water, feces and surfaces, temperature is a significant predictor of half life.  
42 Additionally, it is generally accepted that virus decay is faster at higher humidities but there is some  
43 confusion about whether relative humidity or absolute humidity is a better measure (Shaman and Kohn  
44 2009; Marr et al. 2019). Relative humidity is the ratio of the concentration of water vapour in the air  
45 to the saturation concentration whereas absolute humidity describes the amount of water vapour in a  
46 volume of air (Marr et al. 2019). Absolute humidity is sometimes preferred because it may be a better  
47 predictor than temperature or relative humidity alone (Shaman and Kohn 2009). However, at higher  
48 temperatures, more water can be carried in the air (the absolute humidity can be higher) so the effect  
49 of higher absolute humidities may be confounded by the effects of higher temperatures, making it a  
50 potentially less mechanistic measure. Coronaviruses are also lipid-enveloped viruses so may react similarly  
51 to influenza in response to climate. There may be fewer studies but higher temperatures and higher  
52 relative humidities have been linked with faster breakdown on surfaces (Biryukov et al. 2020), in aerosols  
53 (Doremalen, Bushmaker, and Munster 2013) and in liquids (Chin et al. 2020). In terms of transmission,  
54 experimental evidence has found transmission of influenza between guinea pigs in controlled environments  
55 is higher in colder, less humid environments (Lowen, Mubareka, Steel, et al. 2007). As with viral stability,  
56 some suggest that absolute humidity may be more important than relative humidity or even temperature,  
57 for example the reanalysis of Lowen, Mubareka, Steel, et al. (2007) by Shaman and Kohn (2009).

58 Human behaviour may change with climate due to seasonality in school terms, in particular a long  
59 summer holiday. As some diseases mostly effect children a strong effect of school terms is expected.  
60 Work by Fine and Clarkson (1982) and Finkenstädt and Bryan T. Grenfell (2000) suggests that measles  
61 seasonality may be mediated by school terms. School terms are is also likely to play a role in influenza (J.  
62 Tamerius et al. 2011; Cauchemez, Valleron, et al. 2008) The weather is also likely to impact human contact  
63 rates or type of contacts. Graham and McCurdy (2004) found that in cooler and rainier conditions people

64 spent more time indoors. However there is yet to be work exploring how contact rate changes with time  
65 or attempts to separate the effects of climate on the virus from the effect of climate on human behaviours.

66 Seasonality has frequently been added to SEIR models by modifying the transmissibility of the virus.  
67 Frequently this has been by assuming a sinusoidal shape of transmissibility with time. This has occurred  
68 since work on measles (Bolker and B. T. Grenfell 1993) and more recently (Neher et al. 2020) used it to  
69 explore the potential impact of seasonal forcing on COVID-19. Other work has allowed transmissibility  
70 to vary linearly with temperature, humidity or both (Shi et al. 2020; Postnikov 2016) which will result in  
71 a similar shape if the climate variables change sinusoidally with time. One issue with these models is that  
72 parameterisation is necessary for both the intercept and the effect of climate or time on the transmission  
73 rate which has to be found from data. Brenner, Marwan, and Hoffmann (2017) overcomes this issue by  
74 using experimental data from Lowen, Mubareka, Steel, et al. (2007) reanalysed by Shaman and Kohn  
75 (2009) to find the vapor pressure, a measure of absolute humidity. A lookup table is used to estimate the  
76 transmissibility for a given day (here the transmission rate is a percentage) given the data. This approach  
77 is limited by the data being from guinea pigs, which do not experience the same influenza symptoms as  
78 humans (Lowen, Mubareka, Tumpey, et al. 2006; Julian W. Tang 2009). Changes to contact rate and  
79 diet with climate were not included in the experiment but may effect transmissibility in the real world.  
80 These models are very valuable in improving our understanding of disease dynamics but are limited by  
81 not including the multiple components that may cause seasonality.

82 The majority of the potential causes for seasonality are mediated by climate factors. Although it is  
83 frequently possible to find evidence that certain traits are effected by climate-dependent traits, it can be  
84 difficult to determine whether this is the cause of seasonality so evidence linking climate and disease have  
85 not been able to clarify which factor is the cause. A combination of factors may well be contributing  
86 (Lofgren et al. 2007). Dushoff et al. (2004) suggest that only small fluctuations in transmission with  
87 climate are required for seasonal disease because the similarity between the period of climatic changes and  
88 the intrinsic period of the model (from non-climate dependent factors) allows seasonal disease peaks to  
89 occur due to dynamic resonance. Altizer et al. (2006) demonstrates how the amplitude of the seasonal  
90 forcing may also impact the patterns of disease. Due to this, understanding how the different factors  
91 may interact is really important. For example if one factor leads to better conditions for the virus in  
92 cold temperatures, and another factor leads to better conditions for the virus in warm temperatures, the  
93 amplitude of the seasonal forcing will be much lower than if they peak at the same value. Understanding  
94 the effect of individual components may be useful to understand how interventions can help. For example  
95 social behaviour can be changed but climate cannot, which could be used to manipulate seasonal forcing.

96 Additionally, this knowledge could help us to understand how climate change may impact disease.

97 Transmission is likely to be the major component effected by climate as human behaviour, virus prop-  
98 erties and even some components of human physiology can effect it. Previous work where transmission  
99 varies with time tends to assume a sinusoidal shape without including mechanistic reasoning for this. The  
100 main aim of this project is to explore the effect of temperature on respiratory disease by making a modified  
101 SEIR model to mechanistically model some of the possible causes for temperature dependence of disease.  
102 This will be important in understanding the dynamics of COVID-19 if it were to become endemic. The  
103 aim is to explore the effects of viral decay rate and human contact rate. Contact rate can encompass the  
104 different aspects of human behaviour such as social behaviour and school terms. Virus decay determines  
105 how long a virus can survive in the environment. If the virus cannot survive for long it is less likely to be  
106 transmitted. This offers a mechanistic basis for differences in transmissibility due to climatic conditions.  
107 An important consideration is how human behaviour changes with temperature. Previous work (Mossong  
108 et al. 2008; Hoang et al. 2019) has explored distribution of contact rates in detail. However there is a  
109 lack of high quality data exploring temporal or climatic variation in contact rates. For this reason this  
110 work will explore different scenarios for the temperature at which contact rate is highest, described as the  
111 "mismatch" between the temperatures at which the virus survival and human contact rate are the highest.  
112 Temperature is focussed on as the climate variable of interest here because it has the most clear links with  
113 both behaviour and viral survival. The main aims of this project are:

- 114 - To model the potential effect of temperature dependence of human contacts and virus survival.
- 115 - To find which level of mismatch is most likely and what may determine this.
- 116 - Understand how mismatch effects severity of disease outbreaks.
- 117 - Understand how COVID-19 may behave as an endemic disease.

118 This will be achieved by:

- 119 - Making an SEIR model with a climate dependent transmissible term containing both virus survival and  
120 contact rates as climate-dependent terms.
- 121 - Parameterising this for influenza and simulating the model for many different countries with different  
122 levels of mismatch (different temperatures at which contact rate peaks).
- 123 - Use this data to determine what level of mismatch is the most likely for each country by comparing it  
124 to long term Influenza data
- 125 - Explore  $R_0$  at different levels of mismatch.
- 126 - Using the best mismatch level for each country, estimate the seasonality of COVID-19 and the potential  
127 impact of shifting contact rates.



128



## 129 2 Methods

### 130 2.1 Model

131 The basis of the model is a simple SEIRS model. This is based on models in O. Bjørnstad (2018)  
 132 and Keeling and Rohani (2007). SEIR models are a type of compartmental model which compartments  
 133 for susceptible, exposed (but not yet infected), infected and recovered individuals. SEIRS models are  
 134 modifications of SEIR models where individuals can lose immunity. They are described by a series of  
 135 differential equations, where each differential equation describes the change in the number of individuals  
 in that compartment.

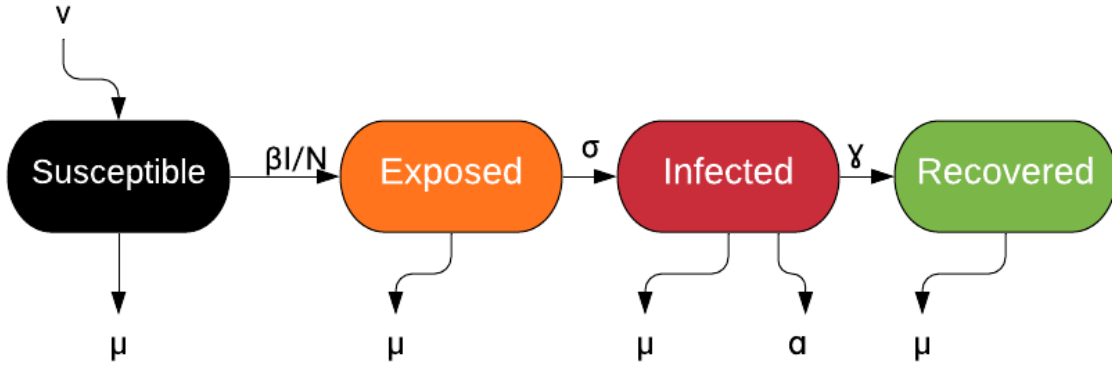


Figure 1: Visual Representation of SEIR model

136

$$\frac{dS}{dt} = \nu N - \frac{\beta IS}{N} - \mu S + fR \quad (1a)$$

$$\frac{dE}{dt} = \frac{\beta IS}{N} - (\sigma + \mu)E \quad (1b)$$

$$\frac{dI}{dt} = \sigma E - (\alpha + \mu + \gamma)I \quad (1c)$$

$$\frac{dR}{dt} = \gamma I - \mu R - fR \quad (1d)$$

137  $\alpha$ , the rate of disease induced mortality, is difficult to parameterise so was replaced by the case fatality  
 138 rate  $p$  as demonstrated by Keeling and Rohani (2007), slightly changing the equation for the change in  
 139 numbers of infectious individuals (2). It is worth noting that disease induced mortality was included

140 (unusual for a typical influenza model) due to the relatively high death rate of COVID-19.

$$\alpha = \frac{p}{1-p} (\mu + \gamma) \quad (2a)$$

$$\frac{dI}{dt} = \sigma E - (\mu + \gamma) \left( \frac{1}{1-p} \right) I \quad (2b)$$

Parameters are described in Table 1.

Parameter	Meaning
S	Number of Susceptible Individuals
E	Number of Exposed Individuals
I	Number of Infected Individuals
R	Number of Recovered Individuals
N	Total Number of Individuals
$\beta$	transmissibility (number of infected individuals per infected individual per day)
$f$	rate of loss of immunity
$\nu$	natural per capita birth rate
$\sigma$	rate of movement from E to I (reciprocal of latent period)
$\mu$	natural per capita death rate
$\gamma$	recovery rate
$\alpha$	disease induced mortality rate
$p$	case fatality rate

Table 1: Basic Parameter meanings for SEIR model. Parameters are described fully (with units and sources) in Table 2 of Supplementary information

141

142 The transmissability ( $\beta$ ) is a climate-dependent term. This model was obtained by modifying the  
143 model in Valle, Hyman, and Chitnis (2013) to add climate dependence. Transmissability is split into  
144 the number of contacts per unit time ( $c_r$ ) and a probability of transmission given a contact between a  
145 susceptible and infected individual. Within this probability there is a climate-dependent term and a scaling  
146 term ( $\epsilon$ ). The climate-dependent term is based on the expected amount of virus in the environment given  
147 a specific duration of contact compared the the amount of virus that would be in the environment after  
148 the time needed for infection to occur (3). It is based on the assumption that the change in the amount  
149 of virus in the environment at time  $t$  is  $a - bV$  where  $a$  is a constant shedding rate,  $b$  is the rate of decay  
150 of the virus and  $V$  is the amount of virus. By integrating this, we can find the the amount of virus at  
151 a time equals to the average duration of contact ( $V = \frac{a}{b}(1 - e^{-bd})$ ). This was divided by itself plus  $ah$ ,  
152 which represents how much virus would be shed in the time required for successful infection to occur ( $h$  is  
153 the expected contact time needed for infection). This cancels to become the fraction in equation 3. This

154 can represent the amount of virus in the environment at a given time considering the rate of decay of the  
 155 virus as a probability of infection.

156 The scaling term covers the multitude of other reasons why  $\beta$  is not the same as  $c_r$  such as the fact that  
 157 risk from contacts vary depending on reasons other than duration and climate, such as type of contact.

158  $\beta = \text{number contacts per unit time} \times \text{probability of disease transmission per contact}$

159

$$\beta = c_r \times \epsilon \times \frac{\frac{1}{b}(1 - e^{-bd})}{\frac{1}{b}(1 - e^{-bd}) + h} \quad (3)$$

160 Climate dependence is included in the model through variation in contact rate ( $c_r$ ) and decay rate ( $b$ )  
 161 of the virus in the environment. In early models, the average duration of contact ( $d$ ) was also climate-  
 162 dependent however the effect of it was minimal.

163 Contact rate as a function of climate was assumed to be based on a normal distribution scaled up  
 164 so the maximum is the maximum contact rate (4). This was calculated for each country such that each  
 165 country was assumed to have the same maximum contact rate. This was done because this work focuses  
 166 on seasonal differences rather than differences between countries. The climate where this peak occurs (i.e.  
 167 the mean of the normal distribution) was not known so 5 values at regular intervals along the climate range  
 168 were modelled. This was converted to the levels of "mismatch" where mismatch is the difference between  
 169 the minimum climate (climate at which survival of the of the virus is highest or viral decay is lowest) and  
 170 the climate at which contact peaks, divided by the maximum possible difference for that climate range  
 171 (see Figure 2a for visualisation of this). A mismatch of 0 means the the contact rate peaks at the lower  
 172 range of the climate variable (which is also where the virus survival is highest and virus decay is lowest).  
 173 The value of  $s$ , the standard deviation of the normal distribution, is determined such that 95% of the  
 174 contact rate of the area under the curve occurs between the minimum and maximum climate. This is  
 175 based on the fact that  $Z = \frac{x-\mu}{s}$  and the z-score required to include 95% is 1.96, where  $x$  is the raw score  
 176 for that z-score. In this case,  $x$  is the upper or lower climate bound ( $\text{max\_}C$  or  $\text{min\_}C$ ). Rearranging  
 177 this gives  $s = \frac{x-\mu}{1.96}$ . The choice of lower versus upper bound is determined by whether the climate of the  
 178 peak contact rate ( $C\_ \text{max\_}c_r$ ) happens closer to the upper or lower bound of the climate. When the  
 179 maximum contact rate happens closer to the lower bound of climate, the maximum is used (4b), otherwise  
 180 the minimum is used (4c).

$$c_r(C) = \text{max\_}c_r \times e^{\frac{-(C - C\_ \text{max\_}c_r)^2}{2s^2}} \quad (4a)$$

181

$$s = \frac{(\text{max\_}C - C\_ \text{max\_}c_r)}{1.96} \quad (4b)$$

$$s = \frac{-(\min\_C - C - \max\_c_r)}{1.96} \quad (4c)$$

Experimental data were obtained for viability of influenza over time in different climatic conditions from Harper (1961). For temperature this was at 7.5, 22.5 and 32 degrees celcius at up to seven timepoints (unless virus had decayed past a detectable level by that point). Where the given temperature or humidity were a range of values (e.g. 21-23 degrees), the mean of this range was used. Exponential decay models (5) were fitted to each set of time series of viabilities using nlsLM in R.  $b$  was bounded between 0 and 5000 per day;  $v_0$  was bounded between 0 and 100%. The Clausius–Clapeyron relation was used to find the absolute humidities for each combination of temperature and relative humidities (as described by Shaman and Kohn (2009)) The decay rates of the virus with temperature, humidity and absolute humidity were fitted to exponential models (6) using nlsLM using the climate values and the  $b$  values found by the earlier model. This obtained an estimate for the rate of decay at time 0 ( $b_0$ ) and the rate of growth of the rate of decay ( $g$ ) with the climate variable. This resulted in equations which could find  $b$  for different climates (for temperature, relative humidity and absolute humidity seperately). Experimental data for SARS-COV-2 and climate were also found (Biryukov et al. 2020). This data contained the half life for eight different combinations of temperature and relative humidity conditions. This was converted into  $b$  by rearranging Equation 5 and setting  $t$  to the half life and  $v$  to equal  $\frac{v_0}{2}$ . nlsLM was used to fit Equation 6 to the climate and  $b$  values.

$$v = v_0 e^{-bt} \quad (5)$$

199

$$b = b_0 e^{gT} \quad (6)$$

## 2.2 Paramaterisation

A literature search was used to estimate parameter values for COVID-19 and Influenza (Table 3 in Supplementary Information).

## 2.3 Data Sources and Sorting

Climate and flu data were obtained from Deyle et al. (2016). This contained relative humidity, absolute humidity, temperature and positive flu results per capita for 79 countries. One country was removed from this because the relative humidities were clearly incorrect. The time was given in the year, month of the year and day of the month (but values were only present up to every week). To simplify analysis this

was converted into week of the year. Only years with 52 or 53 weeks were included so 11090 rows were removed (about 3% of rows). This removed years where only part of the year was known because future averaging steps may have been biased by this. Then the average weekly flu and climate values were found for each country. For each country the minimum, maximum and week of the maximum climate variables were found. This was used to create as a sinusoidal function for the climate for each country (7). This was necessary because weekly time intervals were not sufficient for the integration in later steps.

$$C(t) = \frac{\max\_C - \min\_C}{2} \times \cos\left(\frac{2\pi}{365} \times (t - \text{week\_max\_C})\right) + \frac{\max\_C + \min\_C}{2} \quad (7)$$

Population data was found for these countries from The World Bank (2019). One country was missing population data so was removed from the analysis (French Guinea). Latitude and longitude data was obtained from Google (2019) for each of the remaining countries.

## 2.4 Analytical Sensitivity Analysis

An explicit equation for  $R_0$  was found using an equation from Bjornstad, Finkenstadt, and Greenfell (2002) and modifying it with the previous equation for  $\beta$  (3) and converting from  $\alpha$  to  $p$  (8). SymPy in Python (Meurer et al. 2017) was used to find the partial derivative of  $R_0$  with respect to each parameter. Then this equation was divided by the  $R_0$  equation to find an equation for the change in the parameter as a proportion of  $R_0$  ( $\frac{\partial R_0}{\partial P}$ ). For different parameter combinations for each parameter ( $P$ ) the value of  $\frac{\partial R_0}{\partial P}$  was found by substituting different parameter combinations into this equation.  $q$  and  $c_r$  were assumed to be constant. The temperature range for this was the mean coldest week and the mean hottest week. In addition the temperature where contact rate was highest was set to be the minimum of the temperature range (same value when maximum is used). Then the current temperature was set to the midpoint of the temperature range. Each parameter (including climate dependent parameters) were varied from 50% to 150% of the best estimate of the parameter, at 100 different regularly spaced points.  $\frac{\partial R_0}{\partial P}$  was found for every parameter at each parameter combination (i.e the number of intervals timed by the number of parameters being varied). This was found as both a value and a rank of the relative importance. Over the different parameters,  $h$ ,  $\epsilon$  and  $\mu$  were most frequently the most important parameters. For this reason, these were varied during the integration step. To further test robustness, the analytical sensitivity analysis was repeated with the temperature was set the the lower, middle and upper bound of the temperature range where  $c_r$  and  $q$  were not varied. The results at these three values were very similar. Only the relative importance of  $d$  changed. However as  $d$  was always one of the three least important parameters, this

236 difference could be ignored and the temperature was kept at the midpoint of the range (but  $c_r$  and  $d$   
 237 were still varied as described above).

$$R_0 = \frac{\sigma}{\sigma + \mu} \times \frac{c_r \times \epsilon \times \frac{\frac{1}{b} \times (1 - e^{-bd})}{\frac{1}{b} \times (1 - e^{-bd}) + h}}{(\mu + \gamma) \frac{1}{1-p}} \quad (8)$$

## 238 2.5 Model Simulations

239 Integration was performed for each country for 5 different levels of mismatch. For each country, the  
 240 climate range (used for finding the value of contact rate at different climates) was set to the lowest and  
 241 highest mean weekly temperatures for that country and the population size of the model was set to the  
 242 2019 population of the country. To investigate different levels of mismatch, the integration was repeated  
 243 with the maximum contact rate occurring at different climates, evenly spaced between the higher and  
 244 lower climate values. ode in deSolve in R (with lsoda) Soetaert, Petzoldt, and Setzer (2010) was used  
 245 to integrate the SEIR model over 11 years (intervals of one day) to estimate the number of susceptible,  
 246 exposed, infected and recovered individuals at each time point. The model started with infected (0.1%  
 247 and susceptible 99.9%) individuals. The population size from 2019 was used as the starting population  
 248 for each country. The simulation began at the calendar start of the first year. The values for the first  
 249 year were removed to allow the model to burn in and reduce the impact of the starting time and starting  
 250 values. At each time point the value of the climate variable was found (7). From this the contact rate and  
 251 decay rate were found (Equations 6 and 4). These were used to find the transmissibility ( $\beta$ ), part of the  
 252 SEIR model.  $R_0$  based on these values was found (3).

253 This process was repeated for temperature, relative humidity and absolute humidity.

### 254 2.5.1 Sensitivity Analysis in Integration

255 Many of the parameters used were estimates so some of the parameters were varied and the integration  
 256 repeated for different combinations. The parameters varied were the three most important parameters  
 257 ( $h, \mu$  and  $\epsilon$ ) in the analytical sensitivity analysis and  $f$  which could not be included in the analytical  
 258 sensitivity analysis because it does not contribute to  $R_0$ . Latin hypercube sampling was used to find 160  
 259 combinations of these parameters. "lhs" in R was used to find a values between 0 and 1 given the number  
 260 of repeats and number of parameters. Then "qunif" was used to find the value at which this quantile  
 261 occurred from a uniform distribution between 0.5 and 1.5 times the parameter estimate. This resulted in  
 262 a different parameter combination for each repeat.

263 Additionally the integration was repeated with different values for the standard deviation of  $c_r$ . It was  
264 multiplied by X values between 0.75 and 5 using just the parameter estimates.

## 265 **2.6 Analysis of Integration Results and Data**

266 The mean number of infected individuals and  $R_0$  for each week of the year was found for each integration.  
267 The mean number of positive flu tests per capita each week was found from Deyle et al. (2016) for each  
268 country. The correlation ( $r$ ) between the number of infected individuals and the number of positive flu  
269 tests per capita was found for each level of mismatch, combination of parameters and country to obtain  
270 an approximate value for the similarity between data and model.

## 271 **2.7 COVID-19**

272 For each country, the best mismatch level for influenza was found from the mismatch at which the correla-  
273 tion was highest. The integration was reran using COVID-19 parameters (no sensitivity analysis) with the  
274 best mismatch level for each country for influenza used as the estimated mismatch level for COVID-19.  
275 This was then repeated with different mismatch shifts, where the mismatch was 0.25, 0.5 or 0.75 more than  
276 predicted by the influenza data.

## 277 **2.8 Statistical Analysis**

278 Countries were separated by latitude into temperate and tropics based on whether the absolute value of  
279 their latitude was greater than 23.5. Data analysis was carried out in R and plotting was done using  
280 ggplot2 (Wickham 2016).



## 281 3 Results

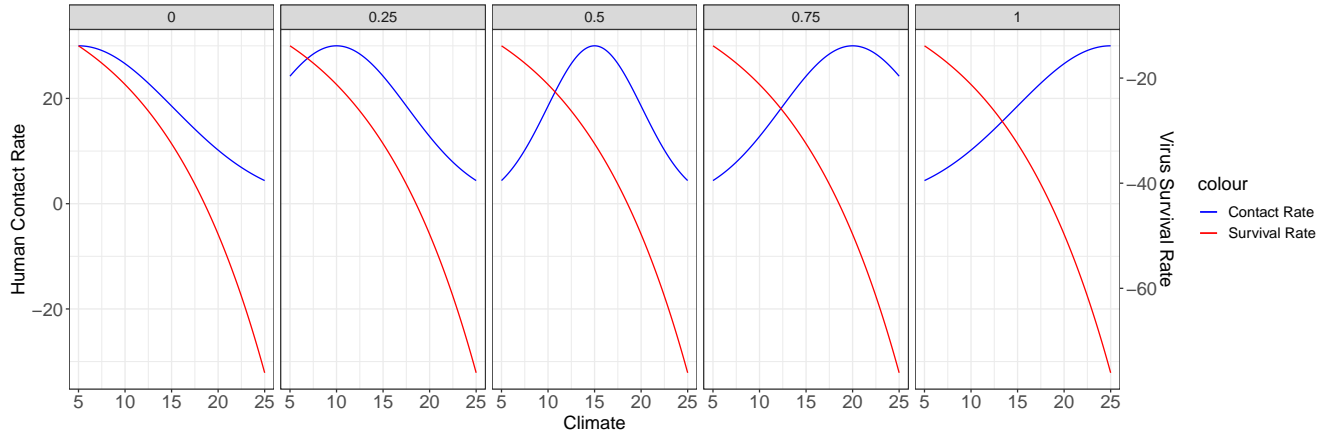
### 282 3.1 Models and Data

283 According to the data, the temperature range was lower in tropical regions (mean: 5.35 degrees, standard  
284 error: 0.64 degrees, n=29) than temperate regions (mean: 20.70 degrees, standard error: 1.12 degrees,  
285 n=48). The virus survival was based on these temperatures and the virus survival range was also lower  
286 in tropical regions (mean difference of 38.12/day between lowest and highest viral decay, standard error:  
287 4.89/day, n=29) than temperate regions (mean difference of 52.88/day, standard error: 3.44/day, n=48).

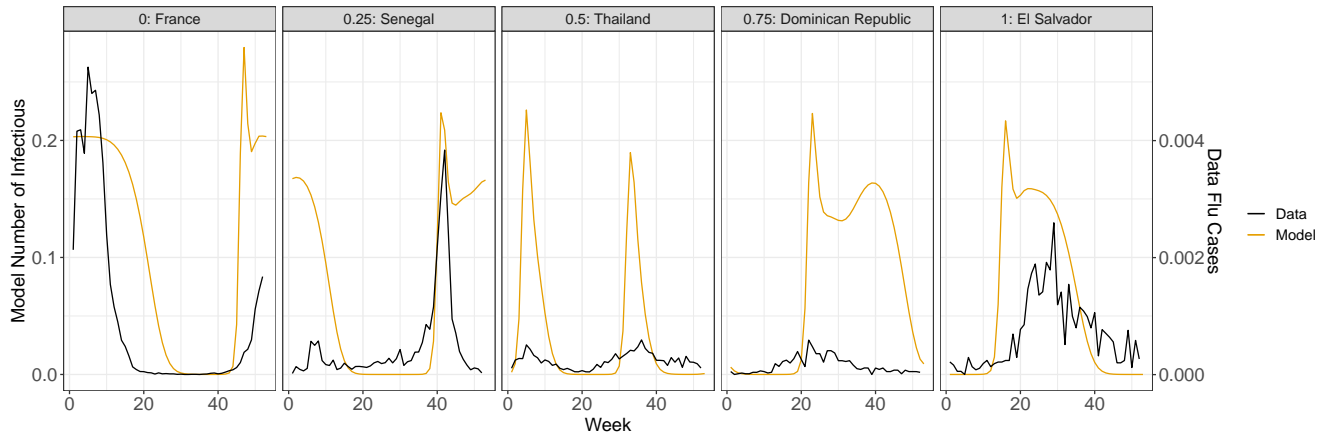
288 The mismatch represents the climate at which contact rate is highest (Figure 2a). Virus Survival rate  
289 is always highest when the climate variable is lowest. A mismatch of 0 means that the survival and the  
290 contact rate are highest at the same climate (so the contact rate peaks at low values). A mismatch of 1  
291 means that the survival and the contact rate are highest at very different values (so the contact rate peaks  
292 at high values). The correlation varied between mismatches meaning that the climate at which contact  
293 rate peaked played a key role in determining how similar the model was to the data. The mismatch level  
294 with the highest correlation varied between countries implying that in different countries, contact rate has  
295 a different relationship with climate (Figure 2).

### 296 3.2 Mismatch and Temperature

297 In the temperate regions, all countries were most similar to models when the contact rate peaked at low  
298 temperatures (46 countries has a mismatch of 0, 2 countries had a mismatch of 0.25). In tropical regions,  
299 the temperature at which contact rate was most likely to peak varied between countries. In 11 countries,  
300 contact rate was highest at low temperatures (mismatch of 0 or 0.25), in 4 countries, contact rate was  
301 highest at intermediate temperatures (mismatch of 0.5) and in 13 countries, contact rate was highest  
302 in high temperatures (mismatch of 0.75 or 1). In temperate regions, the models were better (i.e. the  
303 correlation between the model and data was highest) at low mismatches and worst at high mismatches.  
304 In tropical regions there was not a consistent difference in correlation with different mismatch levels  
305 (Figure 3). Using absolute humidity as the climate variable had the same effect as temperature (Figure 8  
306 in Supplementary information). Using relative humidity as the climate variable led to a weaker effect in  
307 the opposite direction and there was a less pronounced difference between temperate and tropical regions  
308 (8 in Supplementary information). Temperature was focused on for further analysis as it may be linked  
309 more to behaviour. Changing the standard deviation for the contact range does not change the overall  
310 relationships between region and mismatch but the effect becomes less strong (Supplementary Information



(a) Mismatch Visualisation



(b) Data and best model for selected countries

Figure 2: Visualisation for different levels of mismatch. Top panel is the model contact rates and survival rate with temperature for different levels of mismatch. Bottom panel is the number of infectious individuals according to the best model for that country and the mean number of positive flu tests per capita (black). Note: the model and results have different axes because the models and data show very different results, due to both the accuracy of the model and the underestimations of number of flu cases.

Figure 9).

### 3.3 Sensitivity Analysis

Analytical sensitivity analysis found that the most important parameters were  $h, \mu$  and  $\epsilon$  (Figure 4). Further, the results were robust to the variation in parameter values. Figure 3 shows a mean over 100 combinations of parameters. The results are qualitatively the same when just the estimates are used.

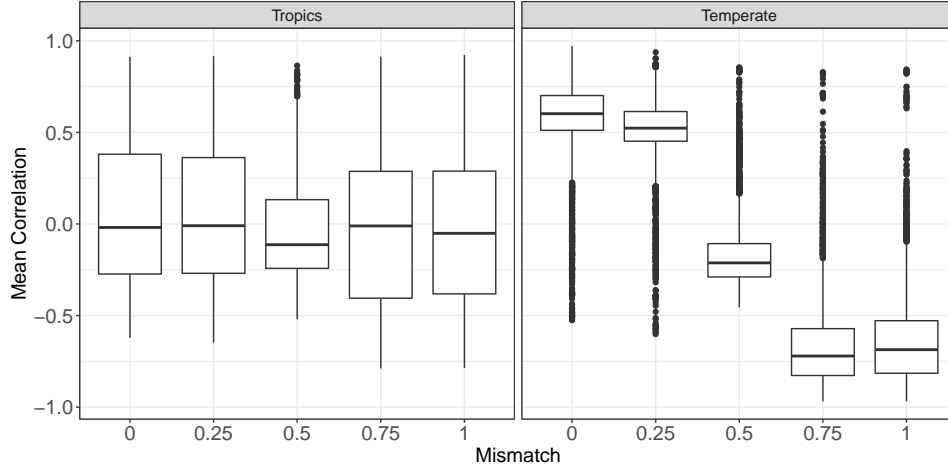


Figure 3: Box and whisker plot of the correlation between data and the model for 5 different mismatches split by whether the country is tropic or temperate. The data is the weekly mean per capita positive influenza tests and the model is the weekly mean proportion of infected individuals. A mismatch of 0 has a higher correlation. n=29 in tropics, 48 in temperate region

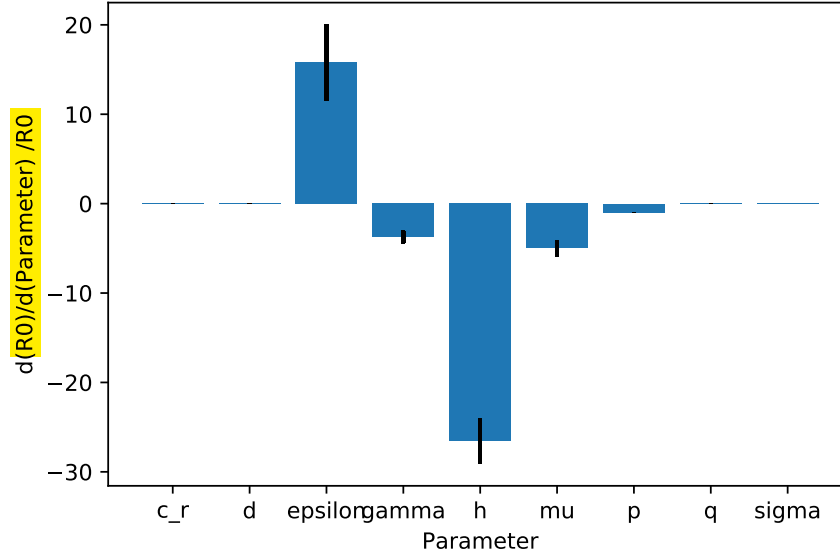


Figure 4: Results of Sensitivity analysis for each parameter in equation 8. Each parameter was varied between 0.5 and 1.5 times the estimated value with 100 intervals and the change in  $R_0$  partial differential of each parameter divided by the  $R_0$  at that point was calculated for each parameter. The mean value for each parameter was plotted with the standard deviation as error bars

### 3.4 Mismatch and Disease Prevalence

In general, tropical countries had lower disease for all levels of mismatch. Models where the contact rate was highest at intermediate temperatures had the lowest mean  $R_0$  and models where the contact rate was

highest at high temperatures had the lowest maximum  $R_0$  (Figure 5).

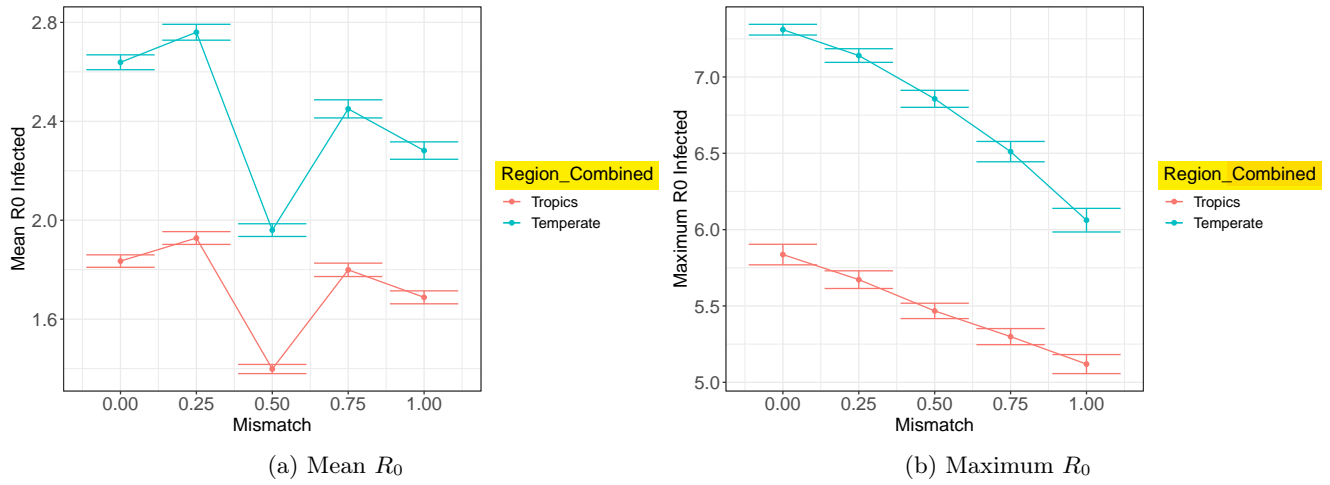


Figure 5: Yearly values of maximum and mean  $R_0$  at different levels of mismatch. In general, values for tropical regions were lower than temperate regions at all mismatches. Mismatches of 0.5 led to the lowest mean values

### 3.5 COVID-19

The COVID-19 model (with mismatch determined by the flu model) suggests one peak of  $R_0$  in the winter of temperate regions although the exact timing does vary (mean is week 9 in northern temperate regions and 29 in southern temperate regions. standard errors are 1.4 and 2.06 weeks respectively). The tropics do not peak at a consistent time (mean is week 29 is and standard error is 2.65 weeks) and often have multiple peaks (Figure ?? in Supplementary Information). Shifting the level of mismatch changes the mean and maximum  $R_0$ . A shift of 0.5 leads to the lowest  $R_0$  in all but 2 of the 48 temperate regions)

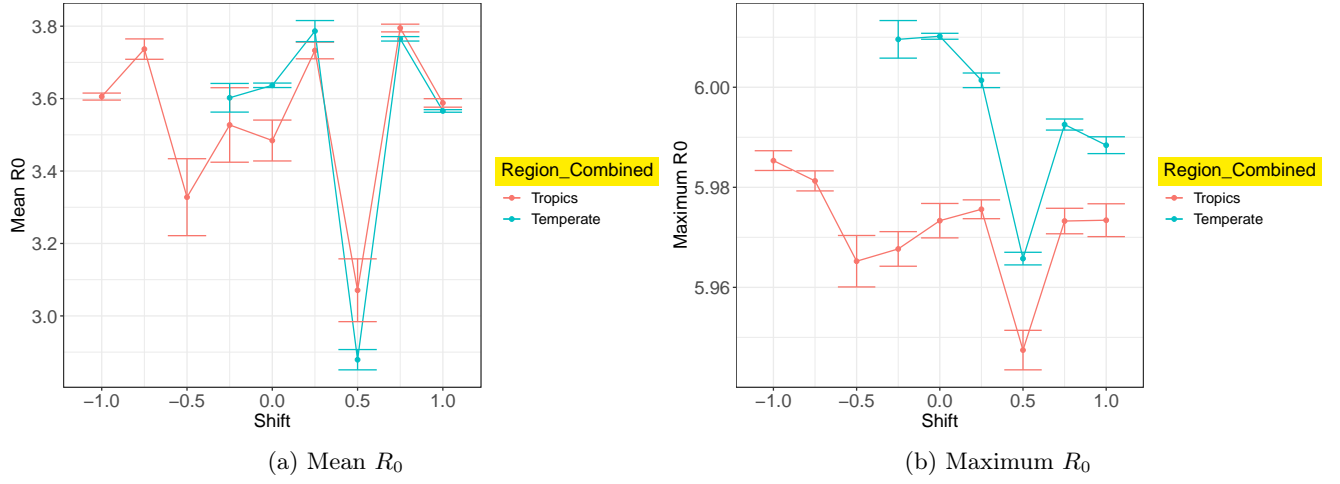


Figure 6: Yearly values of maximum and mean  $R_0$  at different shifted mismatches. A shift of +0.5 decreases the mean and maximum  $R_0$  although the maximum  $R_0$  is not very variable. At a shift of 0 (i.e. mismatch as predicted by the influenza model), the tropics are predicted to have less disease than temperate regions.

## 327 4 Discussion

### 328 4.1 Temperature Findings

329 This work suggests that in temperate regions, contact rate is highest in cooler **temperatures** (i.e. in **Winter**).  
330 This could be due to overall increased contact rate at this time. This could be related to school terms as  
331 winter holidays tend to be shorter than summer holidays and it is clear that schools are a major source of  
332 contacts for children. Cauchemez, Valleron, et al. (2008) found that school holidays prevent almost a fifth  
333 of influenza cases in France. This study only looked at epidemic periods so was not able to pick up the  
334 potential impact of a longer summer holiday on potential for an epidemic. It is worth noting that they did  
335 not find a significant difference between Christmas holidays and other holidays which means the effect of a  
336 religious festival on contact rates may not be important epidemiologically. It is also possible that the result  
337 highlights the role of higher risk or closer contacts which may be more common in winter because more  
338 contacts are indoors. For example, Graham and McCurdy (2004) found that more contacts **are** indoors  
339 in cooler and rainy conditions. Of course if this were the case, viral survival at the outdoor temperature  
340 may be less relevant. The large disparity between temperate and tropical regions is of interest. In the  
341 **tropics**, there is a strong synchrony between contact rates and virus survival, indicated by a mismatch of  
342 0. In tropical regions, this synchrony is not present in most countries. The temperature range changes  
343 with latitude. The tropics have a lower temperature range. In the model, this temperature range effects  
344 the difference between **that** maximum and minimum decay rate. The difference between the maximum  
345 and minimum contact rates in the model are assumed to be consistent between countries but in reality,  
346 in the tropics there may be less variation in contact rates than in temperate regions due to the decreased  
347 temperature range. If this assumption is altered, a more realistic model for contact rate may be obtained.  
348 There are many different possibilities for how temperature might effect contact rate both between and  
349 within countries. Models exploring these can produce insights but for these models to be accurate, data for  
350 how contact rate changes with temperature are needed. The viral survival range does vary with country  
351 in this model. As temperature range is lower in the tropics, range in viral survival is also lower in the  
352 tropics. This may lead to weaker effects of seasonal forcing in the tropics. Dushoff et al. (2004) predicts  
353 that if the intrinsic period of the model is the close to the period of seasonal forcing, resonance between  
354 these factors amplifies the effects of seasonal forcing, even if the effect of seasonal forcing is itself small.

355 In the tropics, there may be differences not included in the model effecting the disparity between  
356 countries. Rain was not included in this model but a rainy season is a common feature of tropical  
357 countries. It is possible that the timing of the rainy season could be determining the timing of contact

358 peaks. Bi et al. (2020) find a link between respiratory virus outbreaks and rainy seasons in the tropics,  
359 although this is not the case for every country.

360 At 0 mismatch, both contact rate and virus survival are highest in low temperatures. This leads to  
361 one clear peak in  $R_0$  when temperature is lowest. At 1 mismatch, contact rate peaks in high temperatures  
362 while virus survival still peaks at low temperatures. This leads to a peak  $R_0$  in high temperatures. This  
363 peak is lower than the peak for 0 mismatch due to the asynchrony. Additionally the  $R_0$  fluctuates over  
364 this period. At a mismatch of 0.5 there are two peaks in  $R_0$  and  $I$  over the course of a year (in between the  
365 amplitude of peaks for 0 and 1 mismatch). These shapes mean that mean  $R_0$  is lowest at an intermediate  
366 mismatch and maximum  $R_0$  being lowest at intermediate mismatches. Countries with a mismatch of  
367 0 peak in cool temperatures and may have the most disease. This is consistent with winter peaks in  
368 temperate regions, which is very common in flu (J. Tamerius et al. 2011). Additionally, across all levels  
369 of mismatch, both maximum and mean  $R_0$  values were lower in the tropics.

## 370 4.2 Different Climate Variables

371 In this study, the results for absolute humidity were very similar to the results for temperature. Absolute  
372 humidity and temperature are linked (Figure 7) and latitude has a strong effect on both temperature and  
373 absolute humidity range. The results for relative humidity showed higher levels of mismatch in temperate  
374 regions (the opposite relationship to absolute humidity and temperature). The best mismatch in temperate  
375 regions was not as consistent. The relationship between temperature and relative humidity may be the  
376 cause for this (Figure 7). The results for both relative humidity and absolute humidity were not any more  
377 insightful than the results for temperature.

378 There may be a complex, non-linear relationship between temperature and humidity (Deyle et al.  
379 2016). Combining multiple climatic variables into the virus survival component of this model could be as  
380 useful way of understanding this relationship more. Additionally temperature may not be the best climate  
381 variable to determine contact rate in the tropics. Rainfall could be incorporated into the contact rate  
382 component. Ultimately, different possible predictors and distributions could be incorporated and model  
383 selection could be used to find which version of the model is most similar to data.

## 384 4.3 COVID-19

385 As for COVID-19, the model predicts a winter peak in temperate regions. This is at odds with what  
386 has been seen in the world, where countries have been affected in all seasons (World Health Organization  
387 (WHO) 2020a). This is likely because when there are high numbers of susceptible individuals, the suscep-

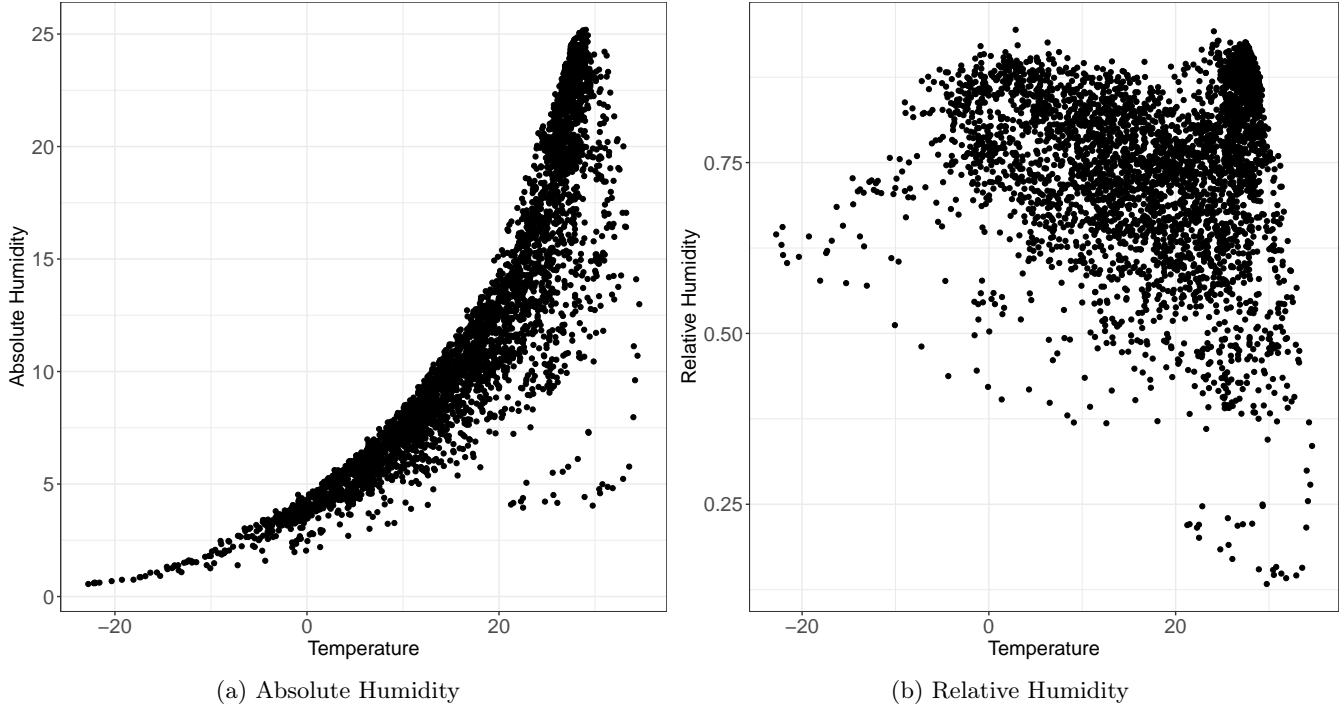


Figure 7: Mean weekly temperatures and humidities from Deyle et al. (2016) dataset. Absolute humidity seems to grow exponentially with temperature, relative humidity is more mixed.

tible supply exerts a stronger effect than seasonal forcing (Baker et al. 2020). That said, some studies have found links between climate variables and severity of COVID-19 (Wang et al. 2020; Luo et al. 2020; Sajadi et al. 2020; Bannister-Tyrrell et al. 2020; Rahman et al. 2020; Oliveiros et al. 2020; Chen et al. 2020; Ma et al. 2020; Poirier et al. 2020) outbreaks but these are very vulnerable to the effects of confounding factors and poor data. While seasonal forcing does not appear to have had a strong effect in early stages of the outbreak, in the longer term, climate may determine when or where outbreaks occur, so understanding the causes for this is likely to be important.

Figure 6 demonstrates that shifting mismatch may effect the severity of outbreaks. Shifting the timing of contact rates could decrease the impact of COVID-19  $R_0$  in the future. In temperate regions, this would be by decreasing contact rates during cold temperatures but allowing them to increase during warmer temperatures. This suggests that reducing winter contacts could reduce the impact of COVID-19 in the long term. Lengthening winter holiday and shortening other holidays could have this effect. Additionally large gatherings could be limited in Winter. There are obviously issues with feasibility of these proposals. In the tropics, shift still appears to decrease the contact rate but for this to be helpful a more detailed understanding of how contact rate varies with climate is necessary. The existing timing of peak contact rate would need to be identified for each country prior to interventions.



#### 404 4.4 Limitations and the Future

405 Due to computing constraints only four different parameters were used as sensitivity analysis when the  
406 simulations were carried out. These were the three parameters that had the greatest impact on an analyti-  
407 cal sensitivity analysis of  $R_0$  and one parameter that could not be included in  $R_0$ . Although the remaining  
408 parameters had a very small effect on  $R_0$  during the sensitivity analysis, its possible that interactions  
409 between parameters would have been different if they were altered in the SEIR model.

410 It is important to note that neither the influenza data nor the model were accurate representations  
411 of the exact numbers of influenza cases. The models were extremely simple. Adding complexity to the  
412 models such as age-dependent contact rates, spatial considerations, variation in mortality and birth rates  
413 between countries would improve this.

414 As J. Tamerius et al. (2011) notes it is imperative to know whether disease transmission is mostly  
415 indoors versus outdoors because this is likely to determine the impact of climate. More research is needed  
416 into contact patterns with climate and time. This data could be very valuable in mitigating respiratory  
417 viruses. If this data could be incorporated into this model, the results would be very valuable. Additionally,  
418 with more time, experimental data for the viruses and climatic conditions could have been combined. At  
419 present only one study was used for influenza and one for COVID-19. A more robust approach would have  
420 been a meta-analysis of all available experimental data. Models are by their nature a simplification of  
421 real life. One potential cause for seasonality that was not included was human physiology and immunity.  
422 The immune system may vary over they year, potentially mediated by vitamin D or by changes in food  
423 availability (J. Tamerius et al. 2011). Additionally, in dryer and potentially cooler environments blood flow  
424 and mucociliary clearance in may lower (J. Tamerius et al. 2011) Additionally, temperature may effect  
425 the shedding rate (Lowen, Mubareka, Steel, et al. 2007). These factors could not be included because  
426 there was not sufficient quantitative information on these effects. More research into these areas is clearly  
427 needed.

428 Understanding these dynamics will particularly useful in predicting the effects of global warming on  
429 respiratory viruses. Understanding how contact rate and virus survival interact may help us to determine  
430 which areas are more at risk from disease outbreaks and put measures in place to detect and prevent these  
431 in the most high risk areas.

432 This work suggests a new model for transmissability as a function of temperature and highlights the  
433 need for more data, particularly the importance of climate-dependent contact data.

## 434 5 Conclusion

435 Previous work acknowledges the importance of seasonality but this is the first work to attempt to untangle  
436 the effects of human behaviour and virus physiology. This model provides a good starting point for the  
437 importance of contact rate and virus survival. The level of mismatch plays a key role in determining  
438 how close the model is to data so this work highlights the need for more research into climate and time-  
439 dependent contact rates. This work was able to estimate the temperature at which contact rate peaks for  
440 each country by comparing model results to data. The result that in temperate regions contact rate is  
441 consistently highest at low temperatures is particularly interesting and could be used to reduce the impact  
442 of respiratory viruses. In the tropics, other climatic variables such as precipitation may be more important  
443 than temperature in determining contact rates. This work offers plenty of avenues for future work.

## 444 References

- 445 Altizer, Sonia et al. (2006). “Seasonality and the dynamics of infectious diseases”. In: *Ecology Letters* 9.4,  
446 pp. 467–484. ISSN: 1461023X. DOI: 10.1111/j.1461-0248.2005.00879.x.
- 447 Baker, Rachel E et al. (2020). “Susceptible supply limits the role of climate in the COVID-19 pandemic”.  
448 In: *Science* 369, pp. 315–319.
- 449 Bannister-Tyrrell, Melanie et al. (2020). “Preliminary evidence that higher temperatures are associated  
450 with lower incidence of COVID-19, for cases reported globally up to 29th February 2020”. In: *medRxiv*  
451 *preprint*.
- 452 Baskerville, Edward B. and Sarah Cobey (2017). “Does influenza drive absolute humidity?” In: *Proceedings*  
453 *of the National Academy of Sciences of the United States of America* 114.12, E2270–E2271. ISSN:  
454 10916490. DOI: 10.1073/pnas.1700369114.
- 455 Bi, Qifang et al. (2020). “Epidemiology and transmission of COVID-19 in 391 cases and 1286 of their close  
456 contacts in Shenzhen, China: a retrospective cohort study”. In: *The Lancet Infectious Diseases* 3099.20,  
457 pp. 1–9. ISSN: 14744457. DOI: 10.1016/S1473-3099(20)30287-5.
- 458 Biryukov, Jennifer et al. (2020). “Increasing temperature and relative humidity accelerates inactivation of  
459 SARS-COV-2 on surfaces”. In: *mSphere* 5.4, pp. 1–9. ISSN: 2379-5042. DOI: 10.1128/mSphere.00441-  
460 20.
- 461 Bjornstad, O.N., Barbel F. Finkenstadt, and Bryan T. Grenfell (2002). “Dynamics of Measles Epidemics  
462 : Estimating Scaling of”. In: *Ecological Monographs* 72.2, pp. 169–184.
- 463 Bjørnstad, Ottar (2018). *Epidemics: Models and data using*, p. 318. ISBN: 9783319974866. DOI: <https://doi.org/10.1007/978-3-319-97487-3>.  
464
- 465 Bjørnstad, Ottar N. and Cecile Viboud (2016). “Timing and periodicity of influenza epidemics”. In: *Pro-*  
466 *ceedings of the National Academy of Sciences of the United States of America* 113.46, pp. 12899–12901.  
467 ISSN: 10916490. DOI: 10.1073/pnas.1616052113.
- 468 Bolker, B. M. and B. T. Grenfell (1993). “Chaos and biological complexity in measles dynamics”. In:  
469 *Proceedings of the Royal Society B: Biological Sciences* 251.1330, pp. 75–81. ISSN: 14712970. DOI:  
470 10.1098/rspb.1993.0011.
- 471 Brenner, Frank, Norbert Marwan, and Peter Hoffmann (2017). “Climate impact on spreading of airborne  
472 infectious diseases: Complex network based modeling of climate influences on influenza like illnesses”.  
473 In: *European Physical Journal: Special Topics* 226.9, pp. 1845–1856. ISSN: 19516401. DOI: 10.1140/  
474 epjst/e2017-70028-2.

475 Cauchemez, Simon, F. Carrat, et al. (2004). “A Bayesian MCMC approach to study transmission of  
476 influenza: Application to household longitudinal data”. In: *Statistics in Medicine* 23.22, pp. 3469–3487.  
477 ISSN: 02776715. DOI: 10.1002/sim.1912.

478 Cauchemez, Simon, Alain Jacques Valleron, et al. (2008). “Estimating the impact of school closure on  
479 influenza transmission from Sentinel data”. In: *Nature* 452.7188, pp. 750–754. ISSN: 14764687. DOI:  
480 10.1038/nature06732.

481 CDC (2020a). *Past Seasons Estimated Influenza Disease Burden*. URL: [https://www.cdc.gov/flu/  
482 about/burden/past-seasons.html](https://www.cdc.gov/flu/about/burden/past-seasons.html).

483 — (2020b). *Public Health Guidance for Community-Related Exposure*. URL: [https://www.cdc.gov/  
484 coronavirus/2019-ncov/php/public-health-recommendations.html](https://www.cdc.gov/coronavirus/2019-ncov/php/public-health-recommendations.html).

485 Chen, Biqing et al. (2020). “Roles of meteorological conditions in COVID-19 transmission on a worldwide  
486 scale”. In: *medRxiv preprint*.

487 Chin, Alex W.H. et al. (2020). “Stability of SARS-CoV-2 in different environmental conditions”. In:  
488 *medRxiv preprint*.

489 Deyle, Ethan R. et al. (2016). “Global environmental drivers of influenza”. In: *Proceedings of the National  
490 Academy of Sciences of the United States of America* 113.46, pp. 13081–13086. ISSN: 10916490. DOI:  
491 10.1073/pnas.1607747113.

492 Doremalen, N. van, T. Bushmaker, and V. J. Munster (2013). “Stability of middle east respiratory syn-  
493 drome coronavirus (MERS-CoV) under different environmental conditions”. In: *Eurosurveillance* 18.38,  
494 pp. 1–4. ISSN: 15607917. DOI: 10.2807/1560-7917.ES2013.18.38.20590.

495 Dowell, Scott F. and Mei Shang Ho (2004). “Seasonality of infectious diseases and severe acute respiratory  
496 syndrome - What we don’t know can hurt us”. In: *Lancet Infectious Diseases* 4.11, pp. 704–708. ISSN:  
497 14733099. DOI: 10.1016/S1473-3099(04)01177-6.

498 Dushoff, Jonathan et al. (2004). “Dynamical resonance can account for seasonality of influenza epidemics”.  
499 In: *Proceedings of the National Academy of Sciences of the United States of America* 101.48, pp. 16915–  
500 16916. ISSN: 00278424. DOI: 10.1073/pnas.0407293101.

501 Ferguson, Neil M. et al. (2005). “Strategies for containing an emerging influenza pandemic in Southeast  
502 Asia”. In: *Nature* 437.7056, pp. 209–214. ISSN: 00280836. DOI: 10.1038/nature04017.

503 Fine, Paul E.M. and Jacqueline A. Clarkson (1982). “Measles in England and Wales - I: An analysis of  
504 factors underlying seasonal patterns”. In: *International Journal of Epidemiology* 11.1, pp. 5–14. ISSN:  
505 03005771. DOI: 10.1093/ije/11.1.5.

506 Finkenstädt, Bärbel F. and Bryan T. Grenfell (2000). “Time series modelling of childhood diseases: A  
507 dynamical systems approach”. In: *Journal of the Royal Statistical Society. Series C: Applied Statistics*  
508 49.2, pp. 187–205. ISSN: 00359254. DOI: 10.1111/1467-9876.00187.

509 Google (2019). *countries*. URL: [https://developers.google.com/public-data/docs/canonical/](https://developers.google.com/public-data/docs/canonical/countries_csv)  
510 [countries\\_csv](https://developers.google.com/public-data/docs/canonical/countries_csv).

511 Graham, Stephen E. and Thomas McCurdy (2004). “Developing meaningful cohorts for human exposure  
512 models”. In: *Journal of Exposure Analysis and Environmental Epidemiology* 14.1, pp. 23–43. ISSN:  
513 10534245. DOI: 10.1038/sj.jea.7500293.

514 Harper, G. J. (1961). “Airborne micro-organisms: Survival tests with four viruses”. In: *Journal of Hygiene*  
515 59.4, pp. 479–486. ISSN: 00221724. DOI: 10.1017/S0022172400039176.

516 Hoang, Thang et al. (2019). “A Systematic Review of Social Contact Surveys to Inform Transmission  
517 Models of Close-contact Infections”. In: *Epidemiology* 30.5, pp. 723–736. ISSN: 15315487. DOI: 10 .  
518 1097/EDE.0000000000001047.

519 Irwin, C. K. et al. (2011). “Using the systematic review methodology to evaluate factors that influence the  
520 persistence of influenza virus in environmental matrices”. In: *Applied and Environmental Microbiology*  
521 77.3, pp. 1049–1060. ISSN: 00992240. DOI: 10.1128/AEM.02733-09.

522 Keeling, Matt J. and Pejman Rohani (2007). *Modeling Infectious Diseases in Humans and Animals*. Prince-  
523 ton, New Jersey: Princeton University Press.

524 Kissler, Stephen et al. (2020). “Projecting the transmission dynamics of SARS-CoV-2 through the post-  
525 pandemic period”. In: *Science*, pp. 1–13.

526 Lauer, Stephen A. et al. (2020). “The Incubation Period of Coronavirus Disease 2019 (COVID-19) From  
527 Publicly Reported Confirmed Cases: Estimation and Application”. In: *Annals of Internal Medicine*  
528 2019. ISSN: 0003-4819. DOI: 10.7326/m20-0504.

529 Lofgren, E. et al. (2007). “Influenza Seasonality: Underlying Causes and Modeling Theories”. In: *Journal*  
530 *of Virology* 81.11, pp. 5429–5436. ISSN: 0022-538X. DOI: 10.1128/jvi.01680-06.

531 Longini, Ira M. et al. (2005). “Containing pandemic influenza at the source”. In: *Science* 309.5737, pp. 1083–  
532 1087. ISSN: 00368075. DOI: 10.1126/science.1115717.

533 Lowen, Anice C., Samira Mubareka, John Steel, et al. (2007). “Influenza virus transmission is dependent  
534 on relative humidity and temperature”. In: *PLoS Pathogens* 3.10, pp. 1470–1476. ISSN: 15537366. DOI:  
535 10.1371/journal.ppat.0030151.

536 Lowen, Anice C., Samira Mubareka, Terrence M. Tumpey, et al. (2006). “The guinea pig as a transmission  
537 model for human influenza viruses”. In: *Proceedings of the National Academy of Sciences of the United*  
538 *States of America* 103.26, pp. 9988–9992. ISSN: 00278424. DOI: 10.1073/pnas.0604157103.

539 Luo, Wei et al. (2020). “The role of absolute humidity on transmission rates of the COVID-19 outbreak”.  
540 In: *medRxiv*, p. 2020.02.12.20022467. DOI: 10.1101/2020.02.12.20022467. URL: <http://medrxiv.org/content/early/2020/02/17/2020.02.12.20022467.abstract>  
541 <https://www.medrxiv.org/content/10.1101/2020.02.12.20022467v1>.  
542 content/10.1101/2020.02.12.20022467v1.

543 Ma, Yueling et al. (2020). “Effects of temperature variation and humidity on the mortality of COVID-19  
544 in Wuhan”. In: *medRxiv preprint*. DOI: 10.1101/2020.03.15.20036426.

545 Marr, Linsey C. et al. (2019). “Mechanistic insights into the effect of humidity on airborne influenza virus  
546 survival, transmission and incidence”. In: *Journal of the Royal Society Interface* 16.150. ISSN: 17425662.  
547 DOI: 10.1098/rsif.2018.0298.

548 Meurer, Aaron et al. (Jan. 2017). “SymPy: symbolic computing in Python”. In: *PeerJ Computer Science* 3,  
549 e103. ISSN: 2376-5992. DOI: 10.7717/peerj-cs.103. URL: <https://doi.org/10.7717/peerj-cs.103>.

550 Mossong, Joël et al. (2008). “Social contacts and mixing patterns relevant to the spread of infectious  
551 diseases”. In: *PLoS Medicine* 5.3, pp. 0381–0391. ISSN: 15491277. DOI: 10.1371/journal.pmed.  
552 0050074.

553 Neher, Richard A. et al. (2020). “Potential impact of seasonal forcing on a SARS-CoV-2 pandemic”. In:  
554 *Swiss medical weekly* 150.3, w20224. ISSN: 14243997. DOI: 10.4414/smw.2020.20224.

555 Oliveiros, B et al. (2020). “Role of temperature and humidity in the modulation of the doubling time of  
556 COVID-19 cases”. In: *medRxiv preprint*. ISSN: 0217751X. DOI: 10.1142/S0217751X20500220.

557 Onder, Graziano, Giovanni Rezza, and Silvio Brusaferro (2020). “Case-Fatality Rate and Characteristics  
558 of Patients Dying in Relation to COVID-19 in Italy”. In: *JAMA - Journal of the American Medical*  
559 *Association* 2019, pp. 2019–2020. ISSN: 15383598. DOI: 10.1001/jama.2020.4683.

560 Poirier, Canelle et al. (2020). “The Role of Environmental Factors on Transmission Rates of the COVID-19  
561 Outbreak: An Initial Assessment in Two Spatial Scales.” In: *SSRN Electronic Journal*. DOI: 10.2139/  
562 ssrn.3552677.

563 Postnikov, Eugene B. (2016). “Dynamical prediction of flu seasonality driven by ambient temperature:  
564 Influenza vs. common cold”. In: *European Physical Journal B* 89.1. ISSN: 14346036. DOI: 10.1140/  
565 epjb/e2015-50845-7.

566 Rahman, Arifur et al. (2020). “A Retrospective Analysis of Influence of Environmental / Air Tem-  
567 perature and Relative Humidity on SARS-CoV-2 Outbreak”. In: *preprints* March. DOI: 10.20944/  
568 preprints202003.0325.v1.

569 Sajadi, Mohammad M et al. (2020). “Temperature, humidity, and latitude analysis to predict potential  
570 spread and seasonality for COVID-19”. In: *SSRN Electronic Journal* 410, pp. 6–7.

571 Shaman, Jeffrey and Melvin Kohn (2009). “Absolute humidity modulates influenza survival, transmission,  
572 and seasonality”. In: *Proceedings of the National Academy of Sciences of the United States of America*  
573 106.9, pp. 3243–3248. ISSN: 00278424. DOI: 10.1073/pnas.0806852106.

574 Shi, Peng et al. (2020). “Impact of temperature on the dynamics of the COVID-19 outbreak in China”.  
575 In: *Science of the Total Environment* January.

576 Soetaert, Karline, Thomas Petzoldt, and R Woodrow Setzer (2010). “Solving Differential Equations in  
577 {R}: Package de{S}olve”. In: *Journal of Statistical Software* 33.9, pp. 1–25. ISSN: 1548-7660. DOI:  
578 10.18637/jss.v033.i09. URL: <http://www.jstatsoft.org/v33/i09>.

579 Sugihara, George, Ethan R. Deyle, and Hao Ye (2017). “Misconceptions about causation with synchrony  
580 and seasonal drivers”. In: *Proceedings of the National Academy of Sciences of the United States of*  
581 *America* 114.12, E2272–E2274. ISSN: 10916490. DOI: 10.1073/pnas.1700998114.

582 Tamerius, James D. et al. (2013). “Environmental Predictors of Seasonal Influenza Epidemics across Tem-  
583 perate and Tropical Climates”. In: *PLoS Pathogens* 9.3. ISSN: 15537366. DOI: 10.1371/journal.ppat.  
584 1003194.

585 Tamerius, James et al. (2011). “Global influenza seasonality: Reconciling patterns across temperate and  
586 tropical regions”. In: *Environmental Health Perspectives* 119.4, pp. 439–445. ISSN: 00916765. DOI: 10.  
587 1289/ehp.1002383.

588 Tang, J. W. et al. (2010). “Incidence of common respiratory viral infections related to climate factors in  
589 hospitalized children in Hong Kong”. In: *Epidemiology and Infection* 138.2, pp. 226–235. ISSN: 09502688.  
590 DOI: 10.1017/S0950268809990410.

591 Tang, Julian W. (2009). “The effect of environmental parameters on the survival of airborne infectious  
592 agents”. In: *Journal of the Royal Society Interface* 6.SUPPL. 6. ISSN: 17425662. DOI: 10.1098/rsif.  
593 2009.0227.focus.

594 The World Bank (2019). *Population*. URL: <https://data.worldbank.org/indicator/SP.POP.TOTL>.

595 United Nations (2019). *World Population Prospects 2019*. URL: <https://population.un.org/wpp/>.

596 Valle, Sara Y. Del, James M. Hyman, and Nakul Chitnis (2013). “Mathematical models of contact patterns  
597 between age groups for predicting the spread of infectious diseases”. In: *Mathematical Biosciences and*  
598 *Engineering* 10.5-6, pp. 1475–1497. ISSN: 15471063. DOI: 10.3934/mbe.2013.10.1475.

599 Wang, Jingyuan et al. (2020). “High Temperature and High Humidity Reduce the Transmission of COVID-  
600 19”. In: *arXiv Populations and Evolution*. DOI: arXiv:2003.05003v1. URL: [http://arxiv.org/abs/](http://arxiv.org/abs/2003.05003?utm_source=researcher_app&utm_medium=referral&utm_campaign=RESR_MRKT_Researcher_inbound)  
601 [2003.05003?utm\\_source=researcher\\_app&utm\\_medium=referral&utm\\_campaign=RESR\\_MRKT\\_](http://arxiv.org/abs/2003.05003?utm_source=researcher_app&utm_medium=referral&utm_campaign=RESR_MRKT_Researcher_inbound)  
602 [Researcher\\_inbound](http://arxiv.org/abs/2003.05003?utm_source=researcher_app&utm_medium=referral&utm_campaign=RESR_MRKT_Researcher_inbound).

603 Wickham, H (2016). *ggplot2: Elegant graphics for data analysis*. New York.

604 World Health Organization (WHO) (2018a). *Influenza (avian and other zoonotic)*. URL: [https://www.](https://www.who.int/news-room/fact-sheets/detail/influenza-(avian-and-other-zoonotic))  
605 [who.int/news-room/fact-sheets/detail/influenza-\(avian-and-other-zoonotic\)](https://www.who.int/news-room/fact-sheets/detail/influenza-(avian-and-other-zoonotic)).

606 — (2018b). *Influenza (seasonal)*. URL: [https://www.who.int/news-room/fact-sheets/detail/](https://www.who.int/news-room/fact-sheets/detail/influenza-(seasonal))  
607 [influenza-\(seasonal\)](https://www.who.int/news-room/fact-sheets/detail/influenza-(seasonal)).

608 — (2020a). *Coronavirus disease 2019 Situation Report -51*. Tech. rep. March. DOI: 10.1001/jama.2020.  
609 2633. URL: <https://www.who.int/emergencies/diseases/novel-coronavirus-2019>.

610 — (2020b). *Novel Coronavirus ( 2019-nCoV ) Situation Report - 1*. Tech. rep.



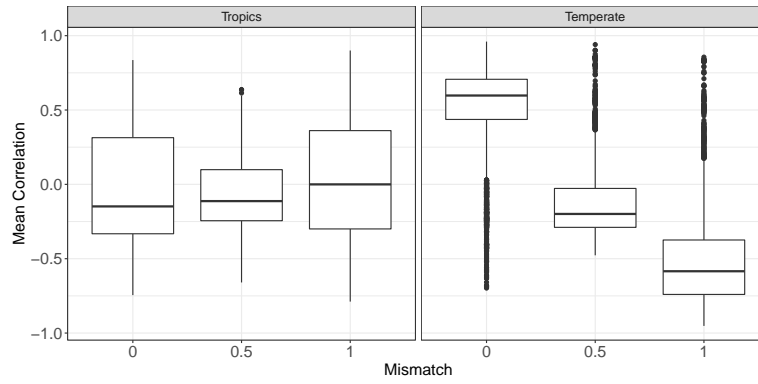
612 **Parameter Meaning Table**

Parameter	Meaning	Unit	Origin
S	Number of Susceptible Individuals	number of individuals(n)	O. Bjørnstad (2018)
E	Number of Exposed Individuals	number of individuals(n)	O. Bjørnstad (2018)
I	Number of Infected Individuals	number of individuals(n)	O. Bjørnstad (2018)
R	Number of Recovered Individuals	number of individuals(n)	O. Bjørnstad (2018)
N	Total Number of Individuals	number of individuals(n)	O. Bjørnstad (2018)
$\beta$	transmissibility (number of infected individuals per infected individual per day)	n/n/day	O. Bjørnstad (2018)
$f$	rate of loss of immunity	1/day	Keeling and Rohani (2007) O. Bjørnstad (2018)
$\nu$	natural per capita birth rate	1/day	
$\sigma$	rate of movement from E to I (reciprocal of latent period)	1/day	
$\mu$	natural per capita death rate	1/day	
$\gamma$	recovery rater	1/day	
$\alpha$	disease induced mortality rate	1/day	
$p$	case fatality rate	-	
$cr$	contact rate per day	n/n/day	Valle, Hyman, and Chitnis (2013)
$\epsilon$	scaling factor as not all contacts lead to successful transmission	-	Valle, Hyman, and Chitnis (2013)
$b$	rate of decay of virus	1/day	Valle, Hyman, and Chitnis (2013)
$d$	average contact duration	days	
$h$	contact duration needed for transmission	days	reciprocal of $\zeta$ Valle, Hyman, and Chitnis (2013)
$T$	Temperature	degrees Celcius	Harper (1961)
$AH$	Absolute humidity	+++	
$RH$	Relative humidity	-	
$s$	standard deviation of contact rate	n/n/day	
$v$	Viability of virus or measure of concentration of virus	%	
$t$	time	day	
$g$	growth constant of decay rate with temperature	1/degrees C	

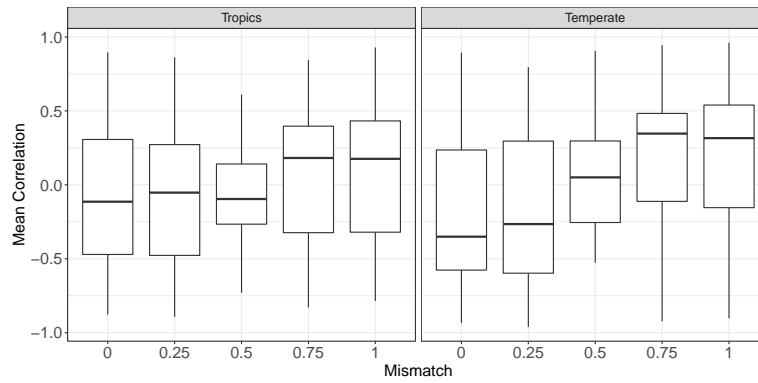
Table 2: Table of model parameters

Parameter	Influenza	Source	COVID-19	Source
$f$	0.1	Estimated by trial and error	0.05	Estimated by trial and error
$\nu$	5.07e-5	Combined mean of countries United Nations (2019)	5.07e-5	combined mean of countries United Nations (2019)
$\sigma$	0.68	Ferguson et al. (2005)	0.2	Lauer et al. (2020)
$\mu$	2.05e-5	Mean of countries United Nations (2019)	2.05e-5	United Nations (2019)
$\gamma$	0.25	Median of Cauchemez, Carrat, et al. (2004) and Longini et al. (2005)	0.048	Bi et al. (2020)
$p$	0.001	Estimated from CDC 2018-2019 data CDC (2020a)	0.01	Onder, Rezza, and Brusaferro (2020)- South Korea
$\epsilon$	0.05	Estimated by trial and error	0.05	Estimated by trial and error
$d$	4/24	Most frequent category of contact duration in polymod study Mossong et al. (2008)	4/24	Most frequent category of contact duration in polymod study Mossong et al. (2008)
$h$	0.25/24	Definition of close contact by CDC CDC (2020b)	0.25/24	Definition of close contact by CDC CDC (2020b)
$\max\_cr$	26.97	Hoang et al. (2019)	26.97	Hoang et al. (2019)
$g$ for T	0.095	From analysis of Harper (1961)	0.078	From analysis of Biryukov et al. (2020)
$b_0$ for T	9.079	From analysis of Harper (1961)	0.256	From analysis of Biryukov et al. (2020)
$g$ for RH	0.0209	From analysis of Harper (1961)		
$b_0$ for RH	21.98	From analysis of Harper (1961)		
$g$ for AH	30.16	From analysis of Harper (1961)		
$b_0$ for AH	0.062	From analysis of Harper (1961)		

Table 3: Table of parameter values. From literature searching and analysis of data in literature.  $b_0$  and  $g$  depend on climate variable so only calculated for influenza (as COVID-19 analysis focuses on temperature).



(a) Absolute Humidity: 1 sample



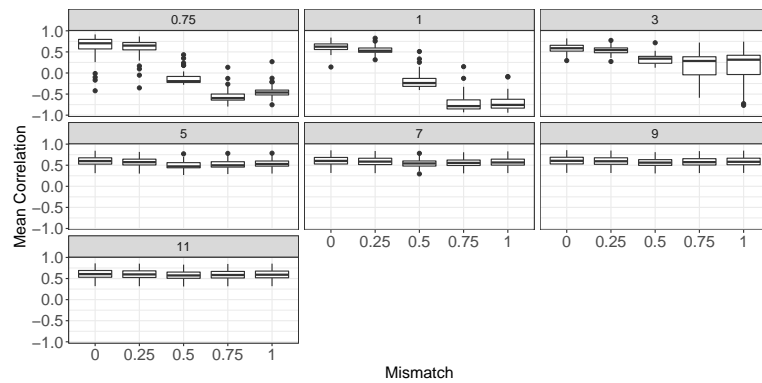
(b) Relative Humidity: 1 sample

Figure 8: Box and whisker plots of the correlation between data and the model for 5 different mismatches split by whether the country is tropic or temperate. The data is the weekly mean per capita positive influenza tests and the model is the weekly mean proportion of infected individuals. A mismatch of 0 has a higher correlation for absolute humidity.  $n=29$  in tropics, 48 in temperate region

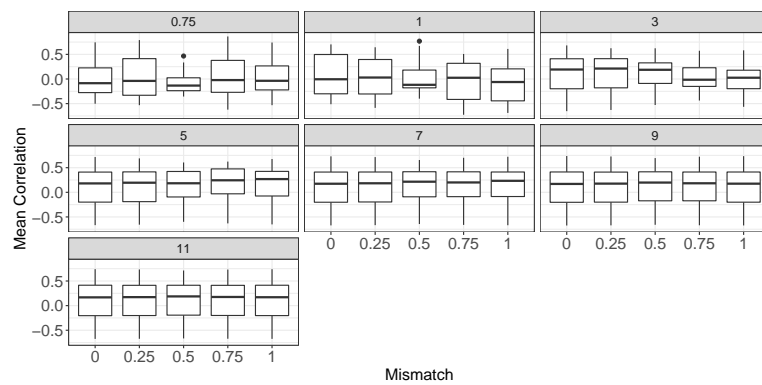
614 **Humidity**

615 **Variance**

616 **5.1 COVID-19 over the year**

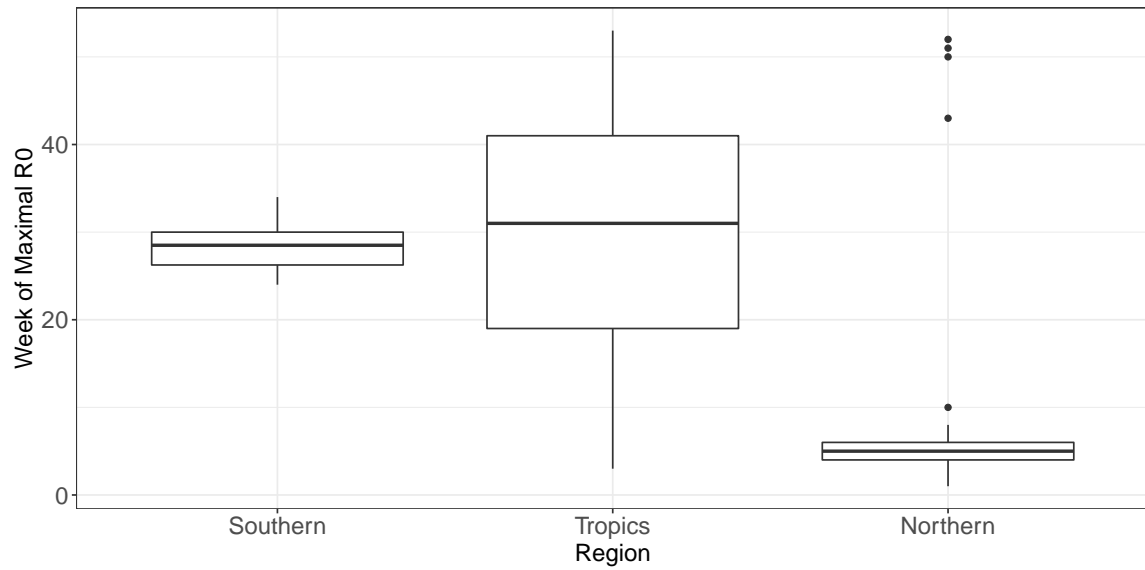


(a) Temperate

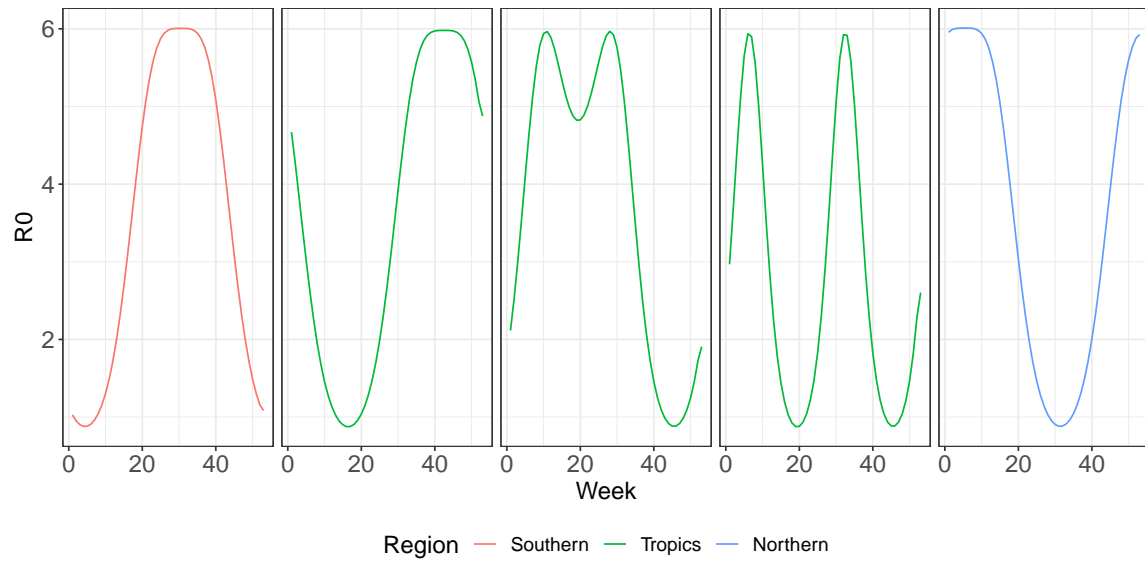


(b) Tropics

Figure 9:



(a) Mean of the week where  $R_0$  is highest for each country for the tropics, northern temperate and southern temperate region.  $n=29$  in tropics, 42 in northern temperate region and 6 in southern temperate region.



(b) Mean  $R_0$  for each week for 5 different countries, representative of each region. Northern and Southern Hemisphere have the same basic shape but in the tropics, there are three different shapes of  $R_0$  over time.

Figure 10:  $R_0$  over time in different regions